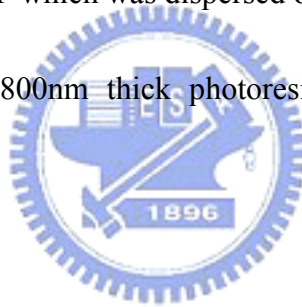


Figure 1. Cross-sectional view of the passivated CNT device. A 300nm Si_3N_4 layer (insulator layer) was deposited on substrate (silicon wafer). After, 100nm metal layer (Titanium) was sputtered as source/drain electrodes. Then, single wall carbon nanotubes is immersed in DMF which was dispersed on the surface of the wafer. After dried at room temperature, 800nm thick photoresist (PR) was patterned as the passivation layer.



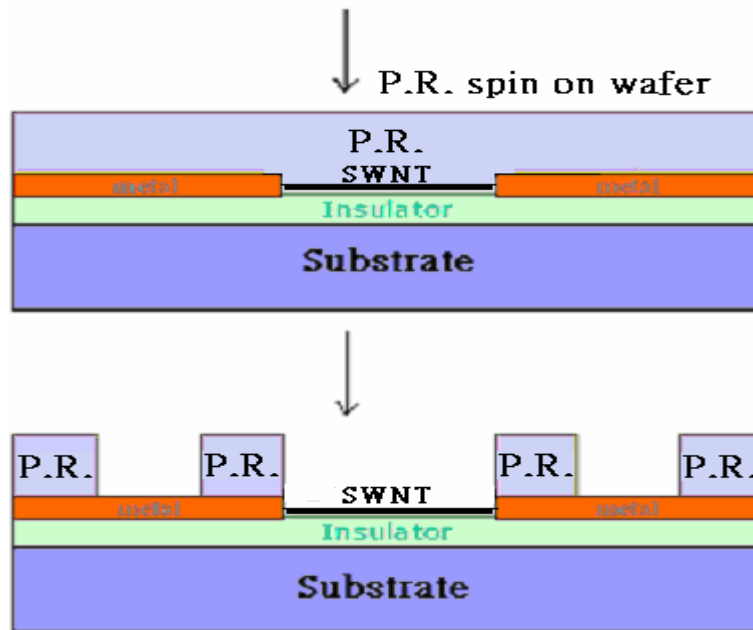


Figure 2. Fabrication of the passivation layer. 800 nm thick photoresist (PR) was laid on the wafer and through patterning, a passivation layer was created over the source/drain electrode. There are three windows which contain two probe pad windows and one sensor window. The passivation layer can prevent the effect of the leakage current.

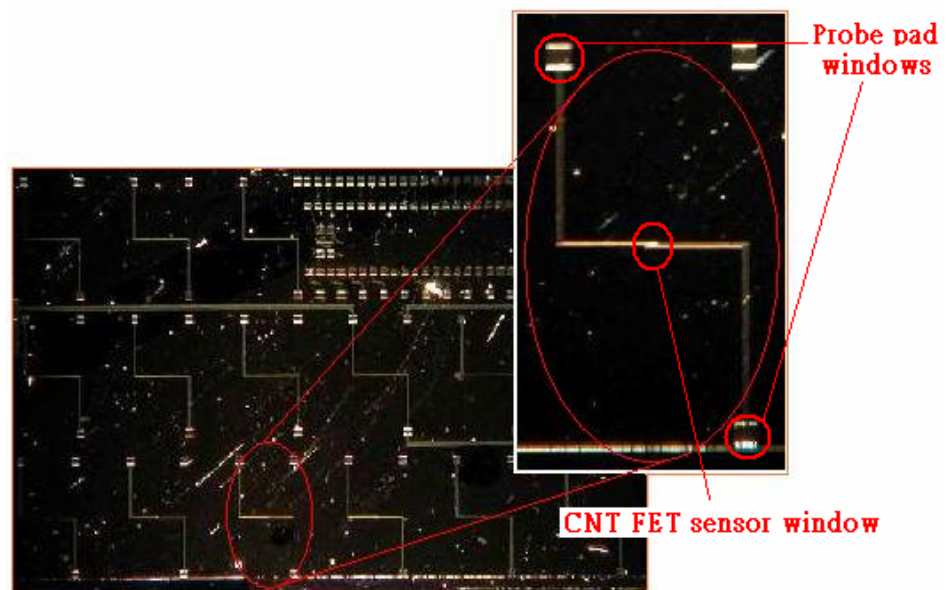


Figure 3. Top view of the CNT device. The chip owns 765 of CNT devices. Each CNT device own two probe pad windows and one sensor window.



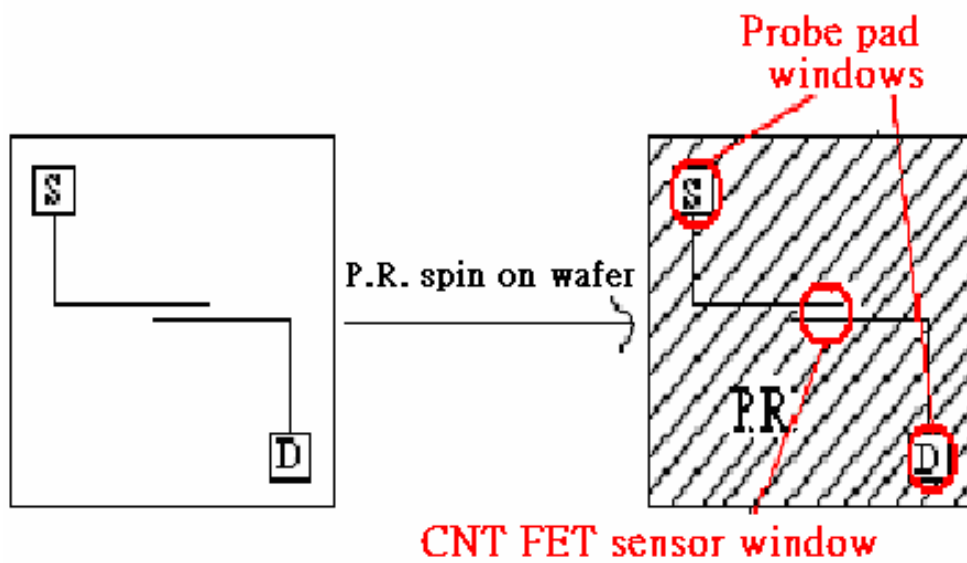


Figure 4. Top view of the passivated CNT device. There are three windows on the passivated CNT device. One is the sensor window and other two are the probe pad windows



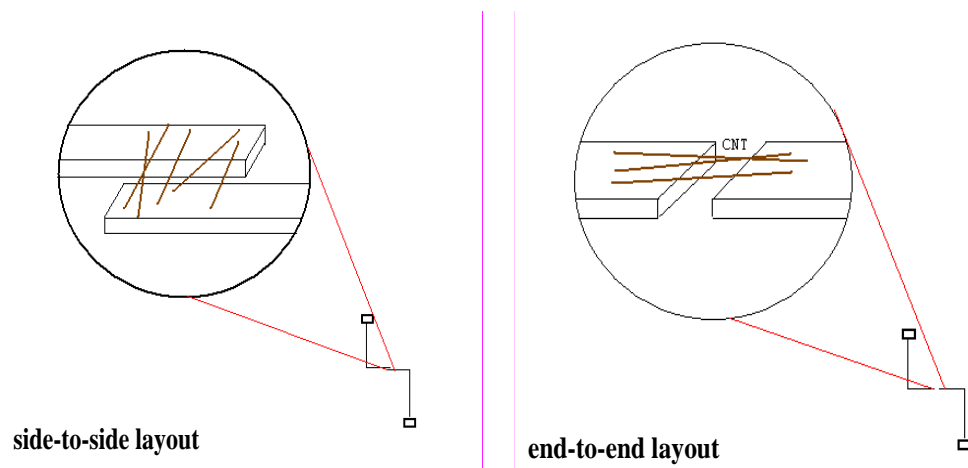


Figure 5. Side-by-side layout and end-to-end layout. The side-by-side layout owns 62 μm length of source/drain electrode for CNT to cross-link. End-to-end layout owns only 2 μm length of electrode.



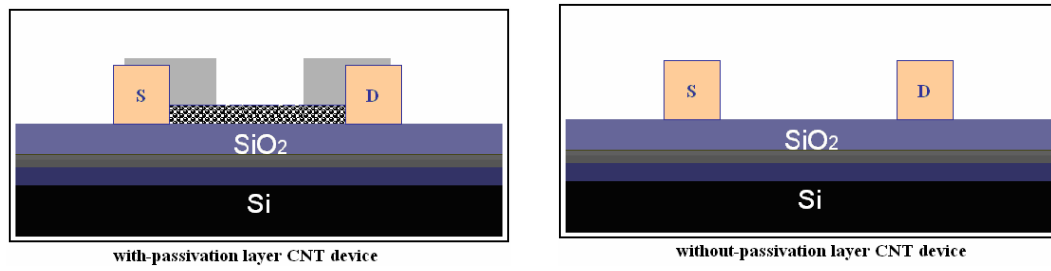
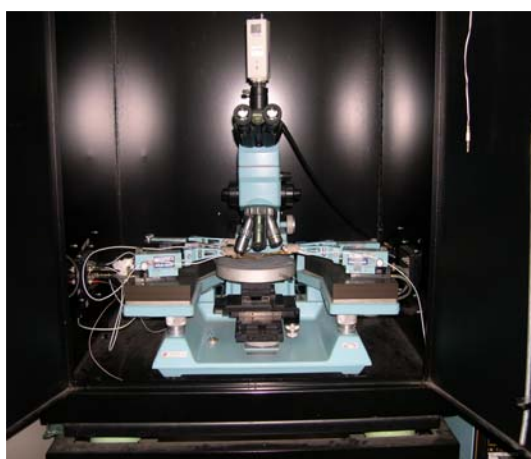
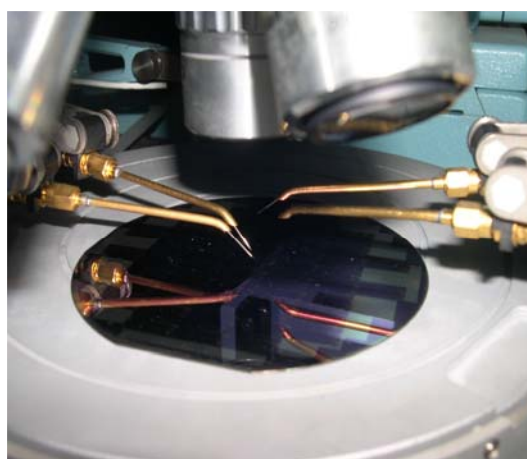


Figure 6. Passivated and non-passivated devices. The passivated CNT devices own 800 μm thick of passivation layer. The non-passivation layer CNT devices have no passivation layer and CNT.





(a)



(b)



(c)



(d)

Figure 7. The instrument of Microscopy , HP 4156 and PC. (a) The shape of microscopy of the analyzer. We can touch the probe to the source/drain electrodes by the microscopy. (b) The picture shows that probe touch to the electrode. (c) The shape of semiconductor parameter analyzer (HP 4156). (d) The data were analyzed by PC.

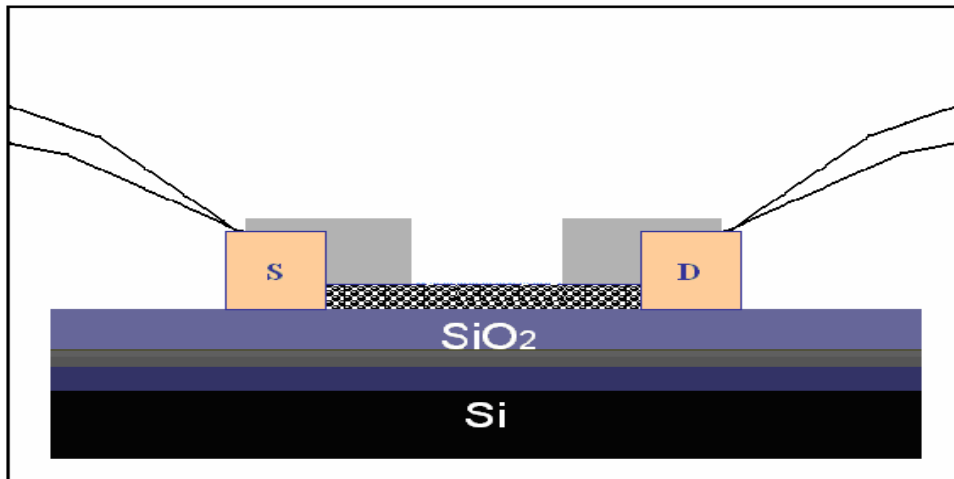


Figure 8. Experiment setup with two-terminal method in ambient air. The probes of the analyzer directly touch to the source/drain electrodes. A drain voltage was supported by the probe of drain. There were no any samples (distilled water and NaCl solution) around the CNT. The method can examines the basic characteristic of the passivated CNT device in ambient air.

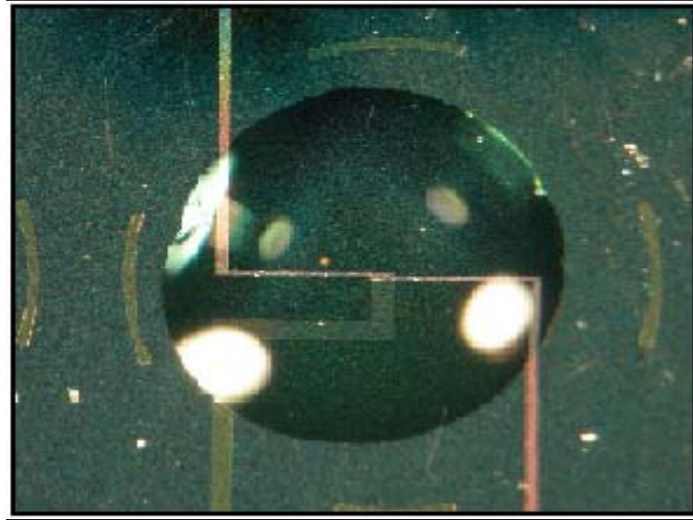


Figure 9. Top view of the small droplet of distilled water and NaCl solution on the CNT device. A micropipette was employed to place a small ($\sim 1\text{--}0.5\ \mu\text{l}$) electrolyte droplet into the sensing window between the source and drain.

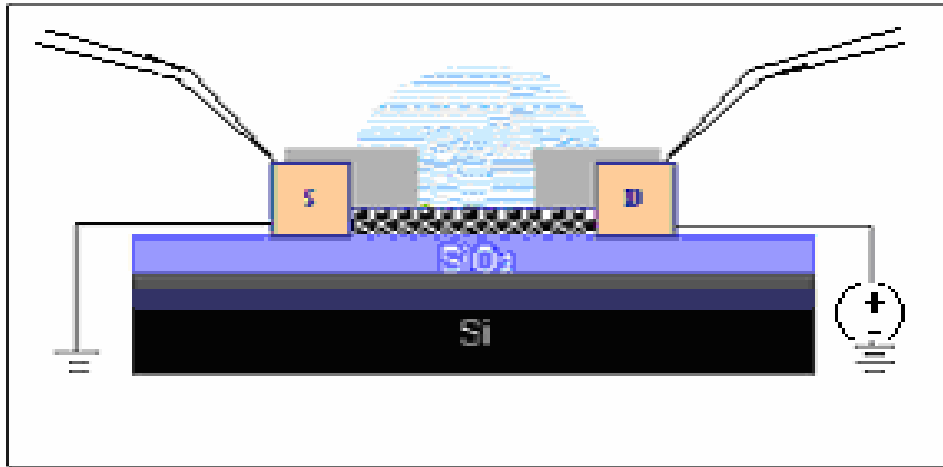


Figure 10. Experiment setup with two-terminal method in aqueous solution.

Deionized water and NaCl solution were assed into the sensor window, respectively.

The solution will affect the ambient environment of CNT. The result will change the signal of the measurement current.

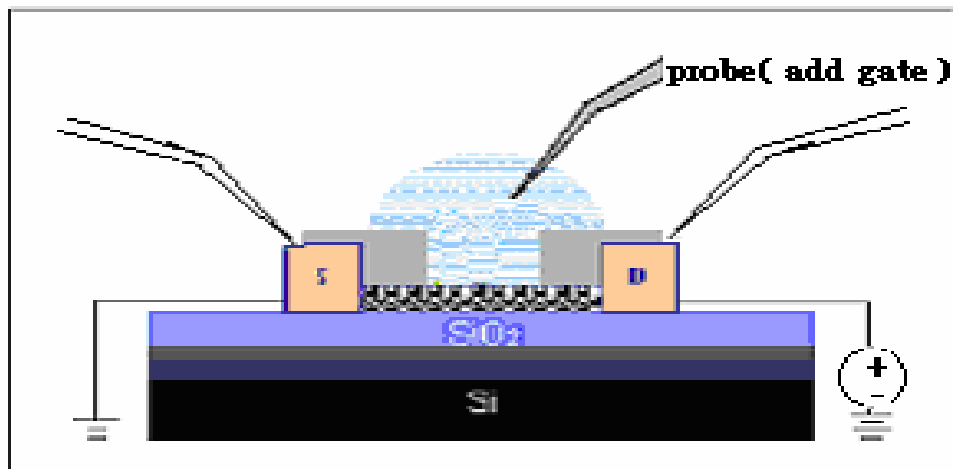


Figure 11. Experiment setup with an adding liquid-gate electrode in aqueous solution. The probe that acts as gate in the experiment was immersed in the solution.

A special voltage was added through the adding gate.



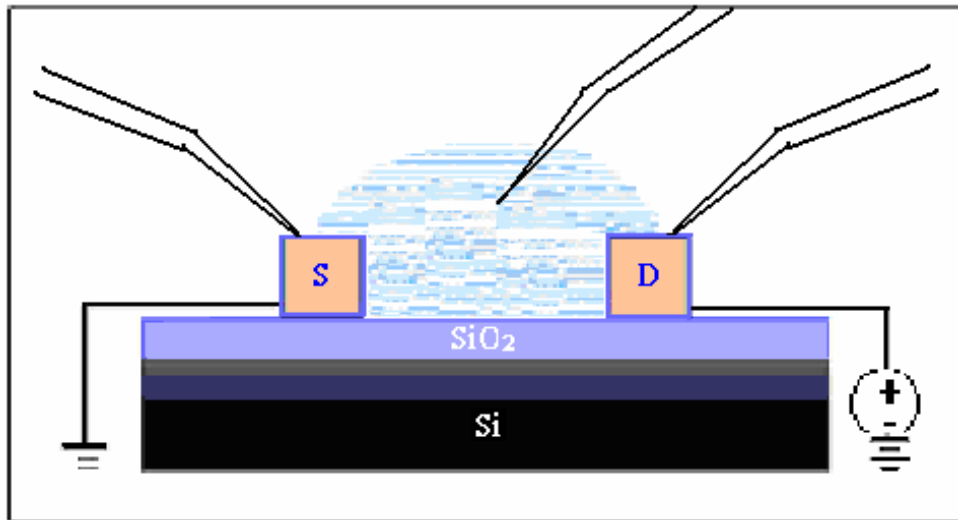


Figure 12. Experiment setup with non-passivated CNT device. There had no passivation layer on the CNT device. The leakage current directly influences the measurement current.



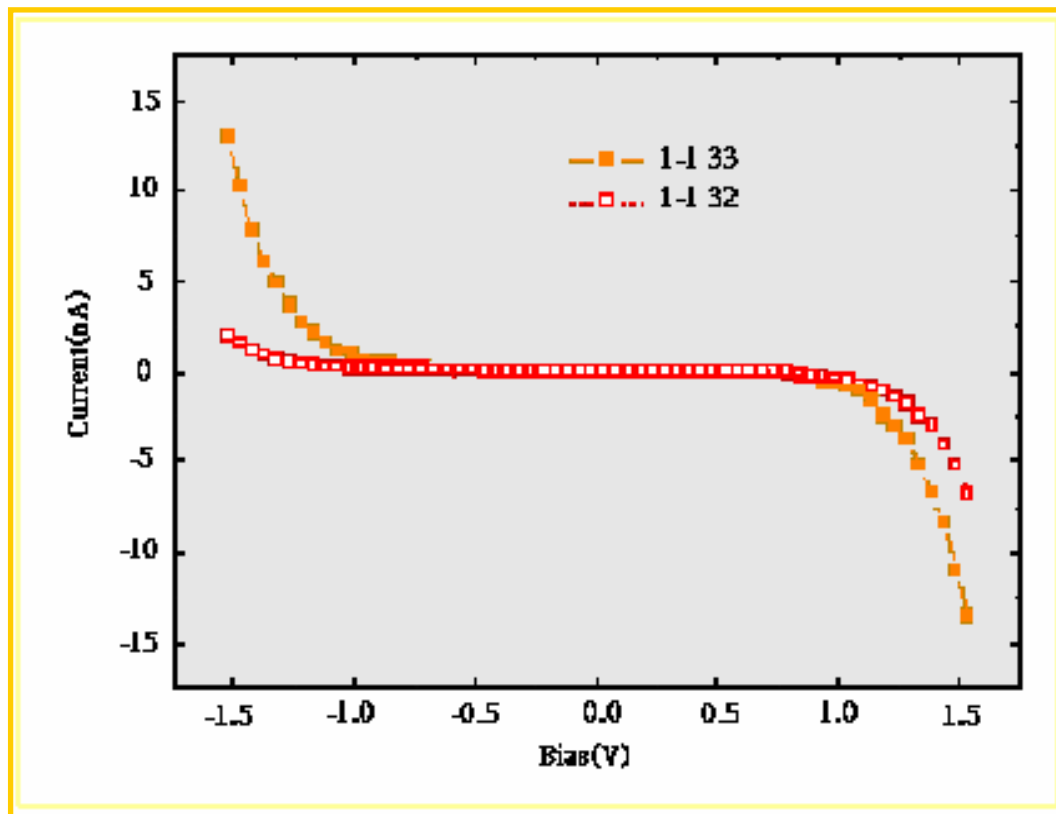


Figure 13. I-V curves illustrated the basic property of the passivated CNT device.

The CNT device has a typical fashion of I-V curve. Here, the data also illustrate that

1-1 33 and 1-1 32 are different from the basic properties.

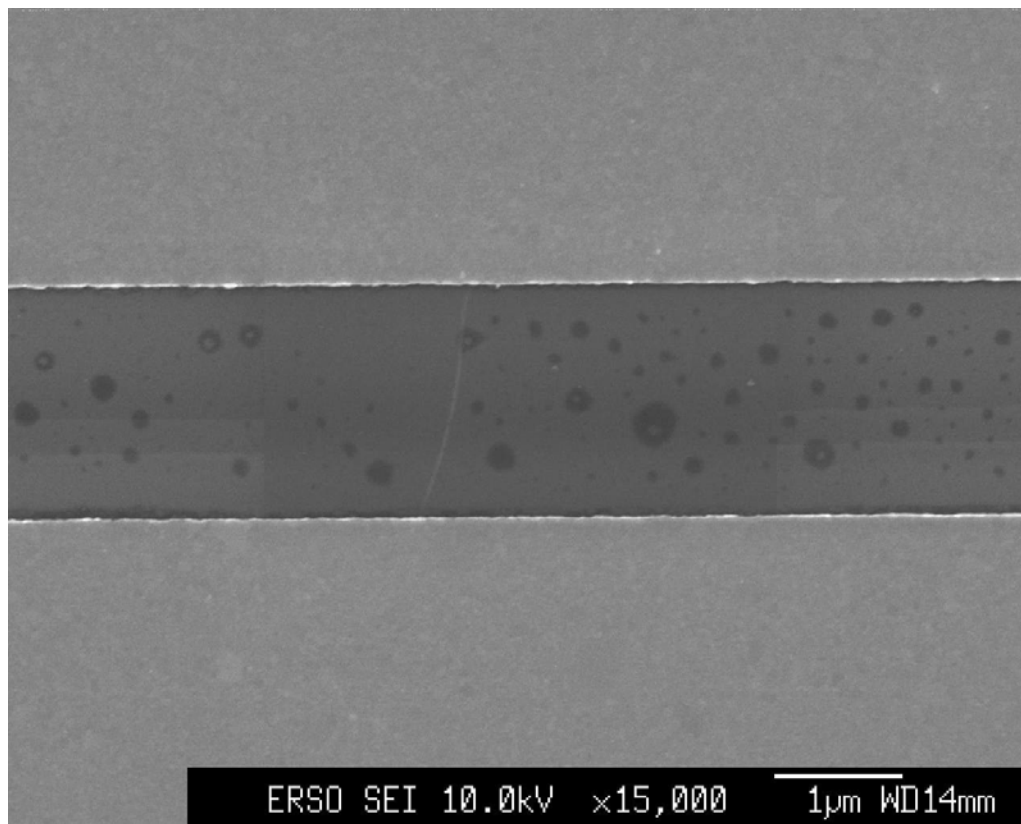


Figure 14. AFM image of CNT in the sensor window. The AFM presented the diameter of the CNT is 1.4nm and the length between two pads is 2 μm .

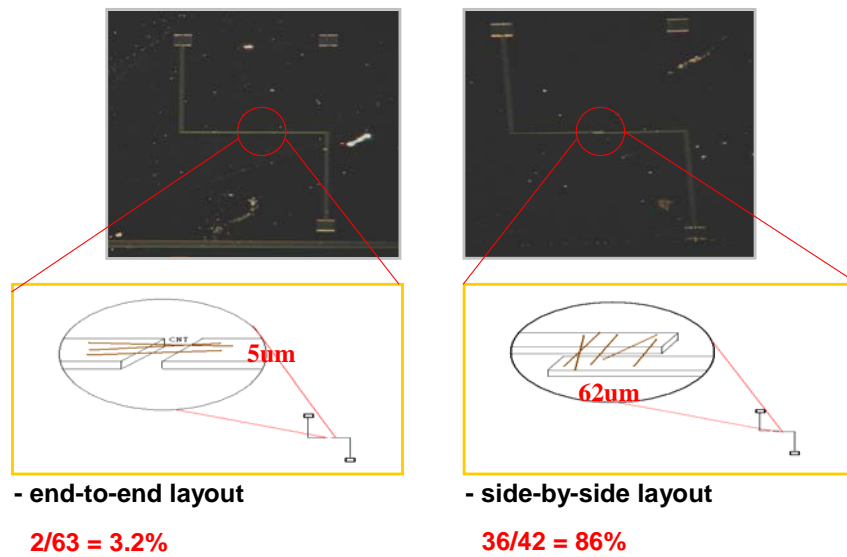


Figure 15. Operative ratio between end-to-end and side-by-side layout. The side-by-side devices have higher operative ratio of 86% than the 3.2% of the end-to-end layout.

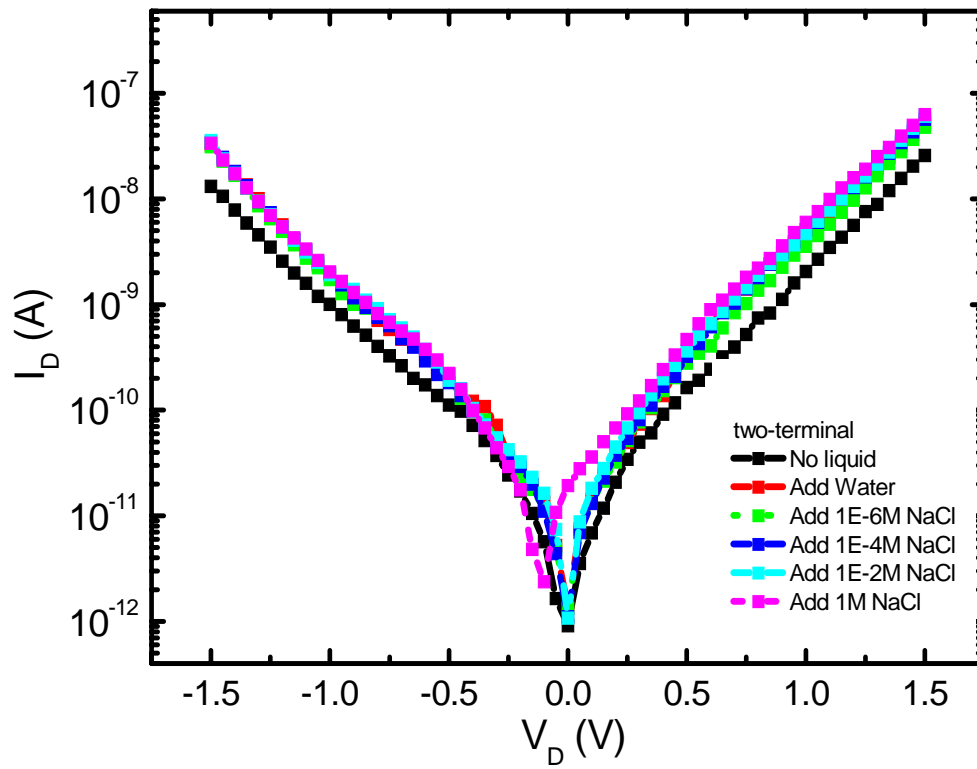


Figure 16. I-V curves of different solution by two-terminal method. I_D - V_D curve varieties was observed by dropping distilled water (resistivity $\sim 18.2 \text{ M}\Omega\text{-cm}$) and NaCl solution (from $1 \times 10^{-6} \text{ M}$ to 1 M) into the sensor window by two-terminal method.

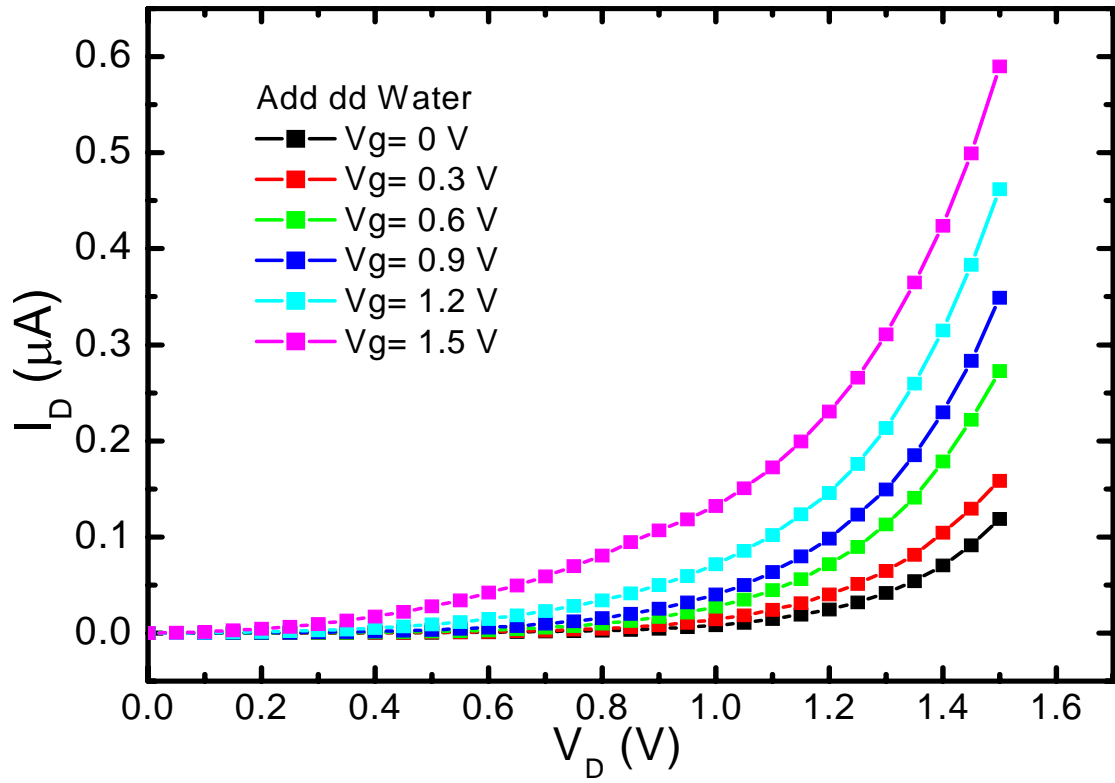


Figure 17. I-V curves illustrated the FET property in deionized water by three-terminal method. The measured current for CNTs exposed to the distilled water by applying different voltage on liquid-gate.

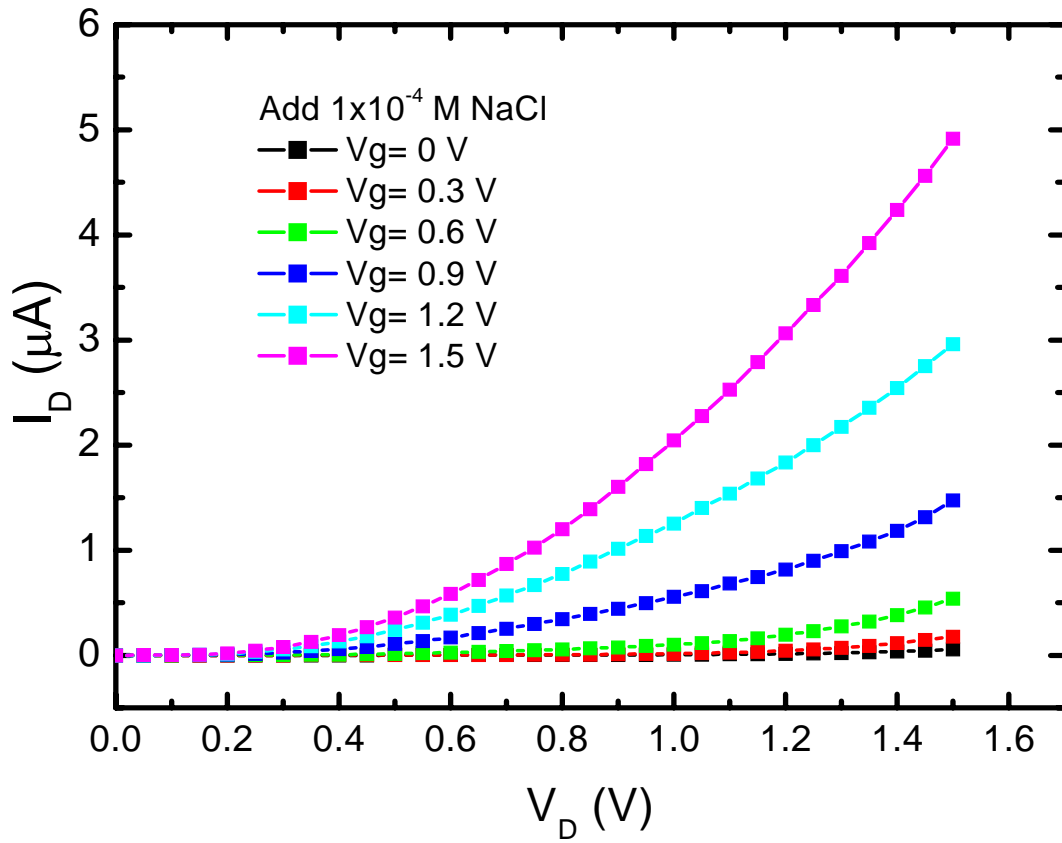


Figure 18. I-V curves illustrated the FET property in NaCl solution by three-terminal method. The measured current for CNTs exposed to the NaCl solution by applying different voltage on liquid-gate.

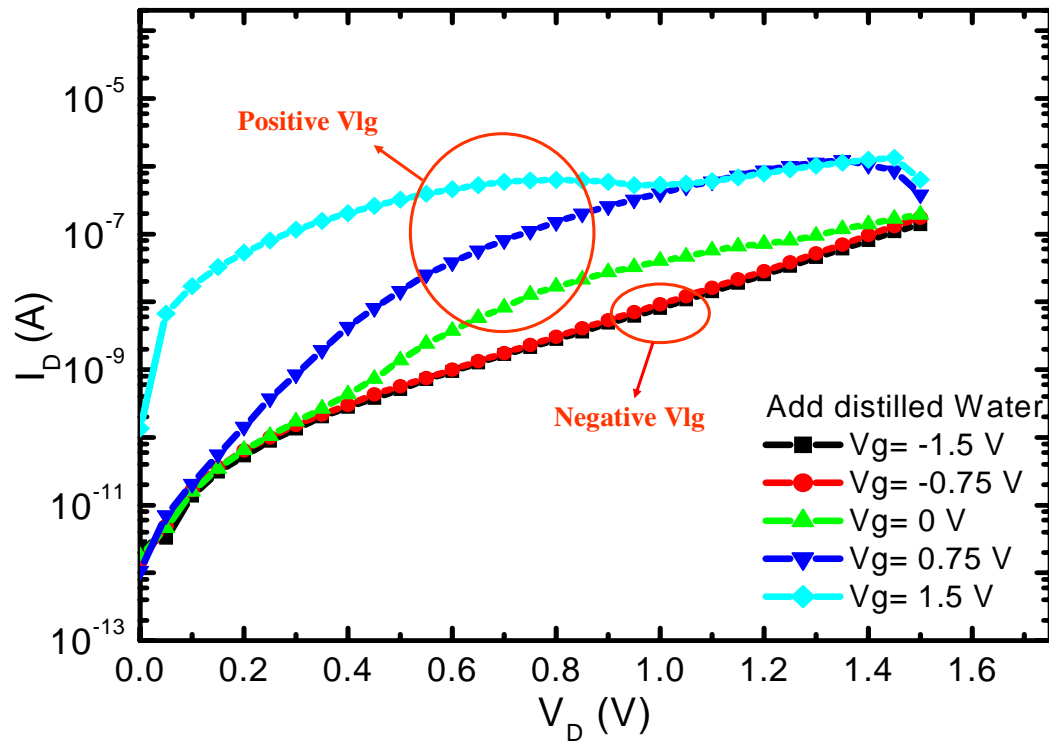


Figure 19. Data demonstrated the I-V curves by supplying positive and negative Vlg. The measured current for CNTs exposed to the distilled water by applying different voltage from -1.5V to 1.5V.

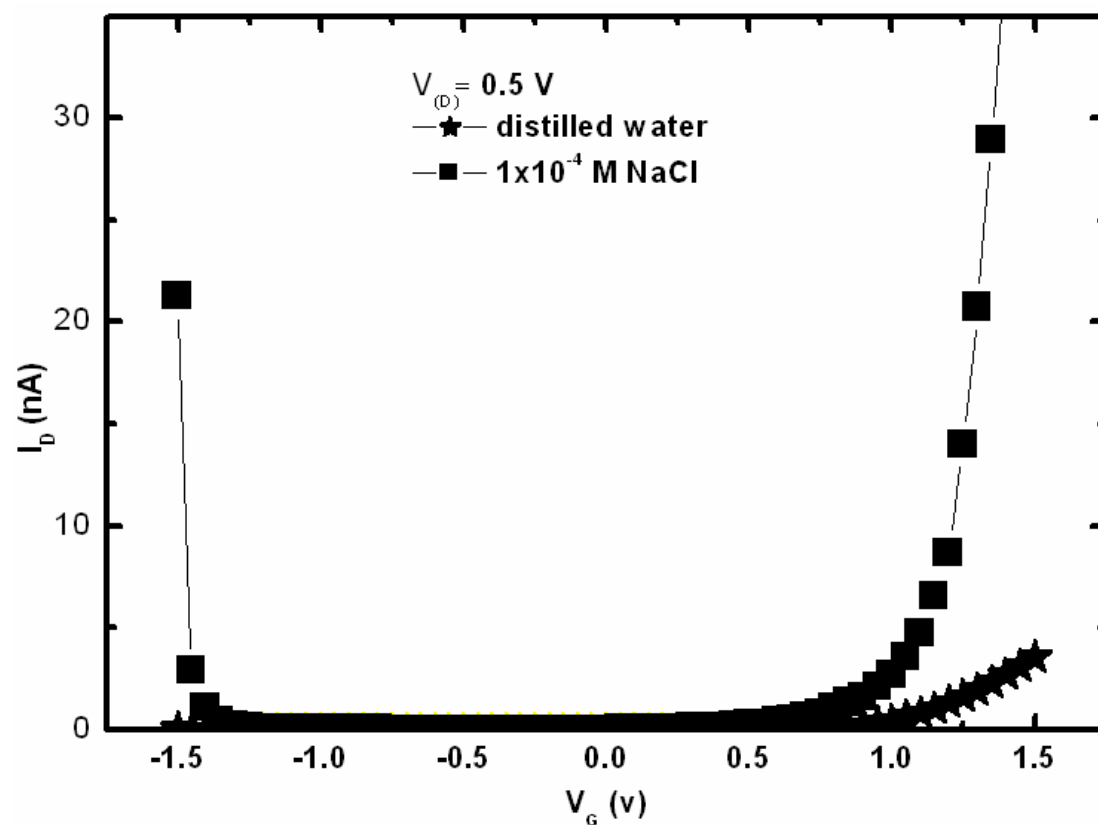


Figure 20. Data show the turn on voltage of positive and negative V_G . The measured current for CNTs exposed to the distilled water (★) and aqueous solution (■) at 0.5 V of drain voltage.

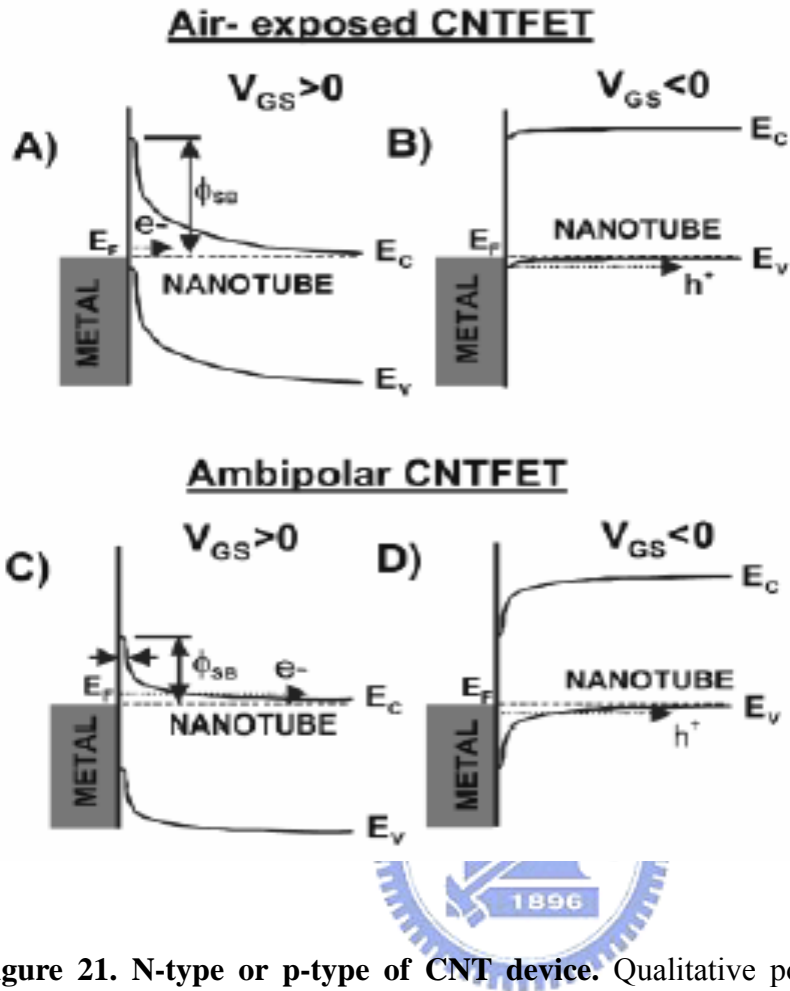


Figure 21. N-type or p-type of CNT device. Qualitative potential energy curves showing the bending of a semiconducting nanotube valence and conduction bands near the nanotube/metal interface. Curves A and B show the bandbending in air (p-CNTFET), whereas curves C and D depict the behavior of an ambipolar CNTFET.

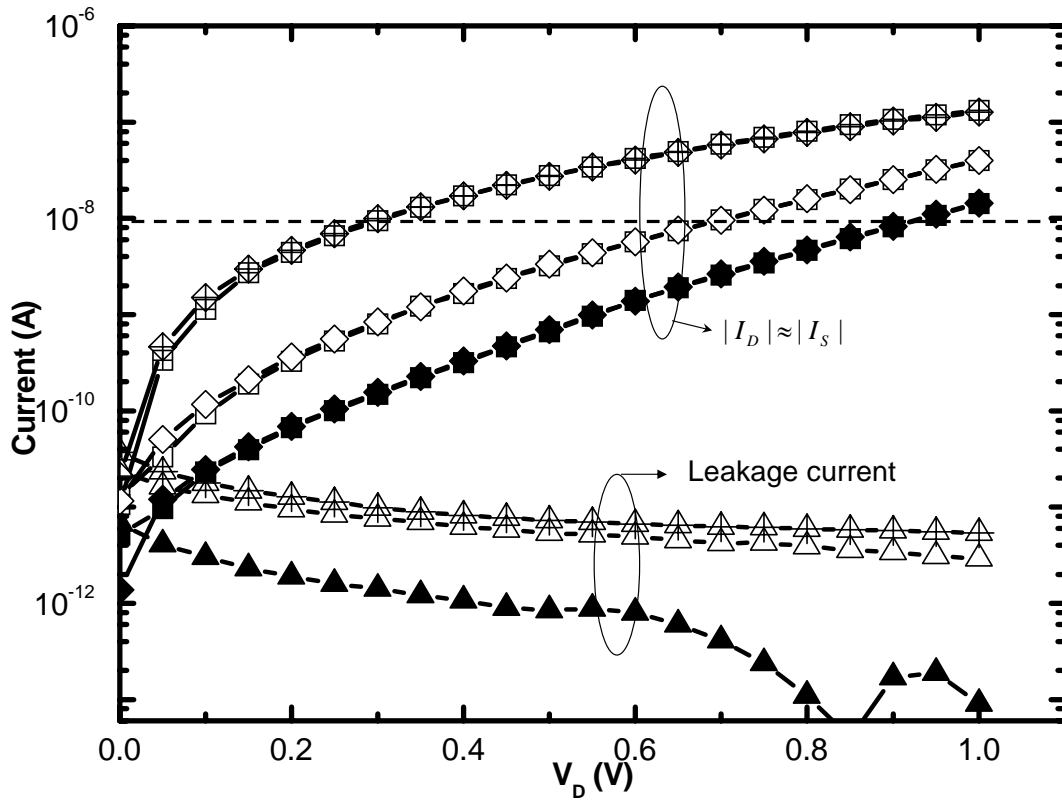


Figure 22. The relationship between the measured drain and the leakage current in distilled water. Data show the measured drain, source and leakage current versus V_D for $V_{lg} = 0.3, 0.9$, and 1.5 V.

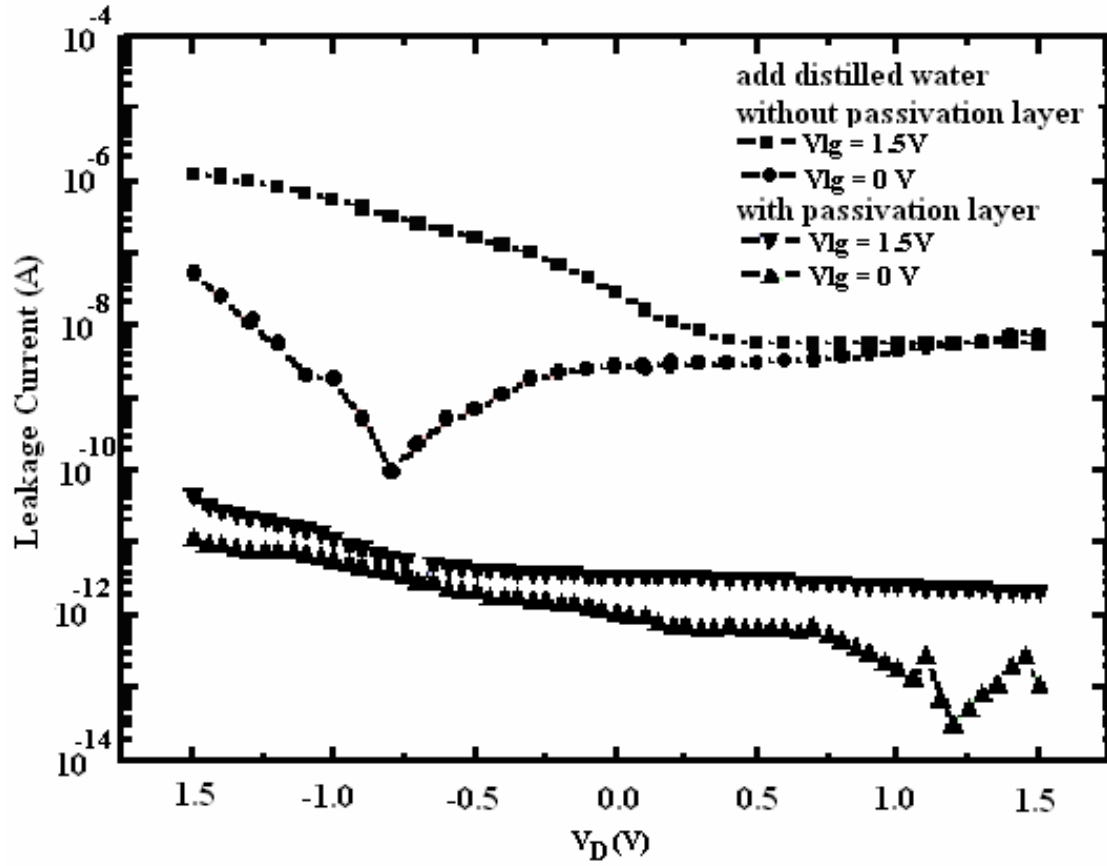


Figure 23. Comparison of leakage currents between passivated and non-passivated CNT devices in deionized water. Data for the With- passivated device exposed to the distilled water (■ for $V_{lg} = 1.5\text{ V}$, ● for $V_{lg} = 0.0\text{ V}$) and Without- passivated device (▼ for $V_{lg} = 1.5\text{ V}$, ▲ for $V_{lg} = 0.0\text{ V}$).

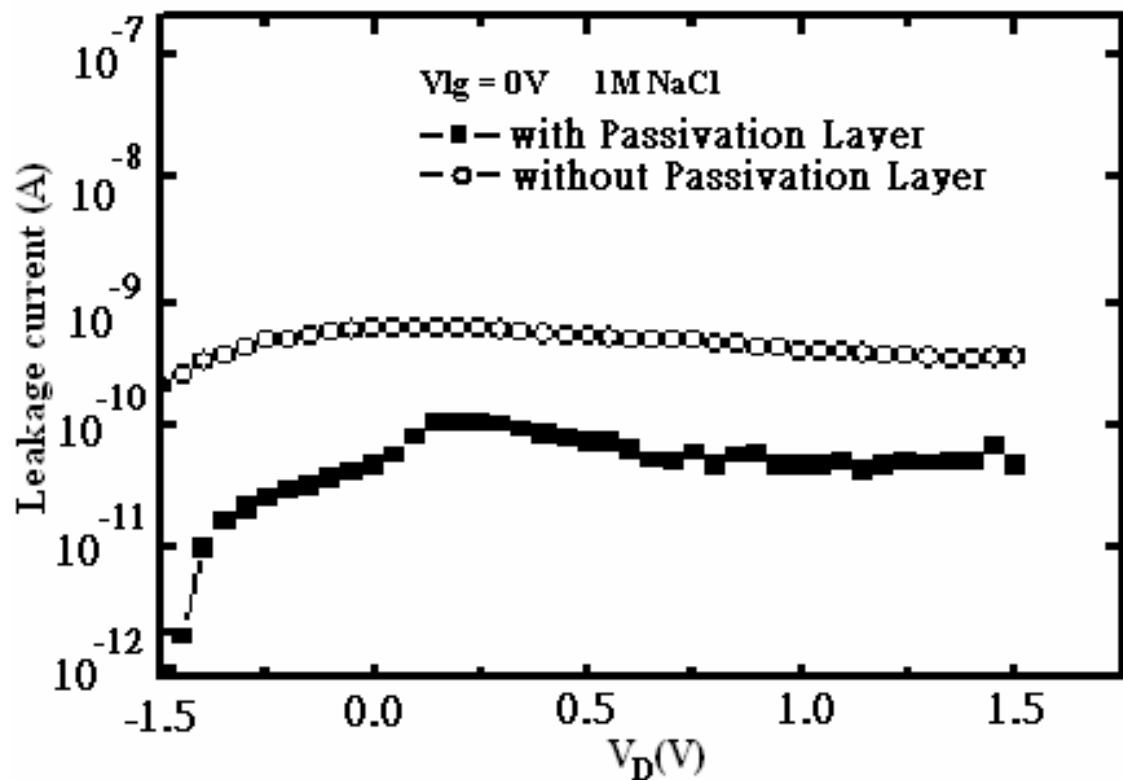


Figure 24. Comparison of leakage currents between passivated and non-passivated CNT devices in NaCl solution. The liquid-gate voltage was kept constant at 0V for the measurement. Data for the passivated device (circle), the non-passivated device (square).

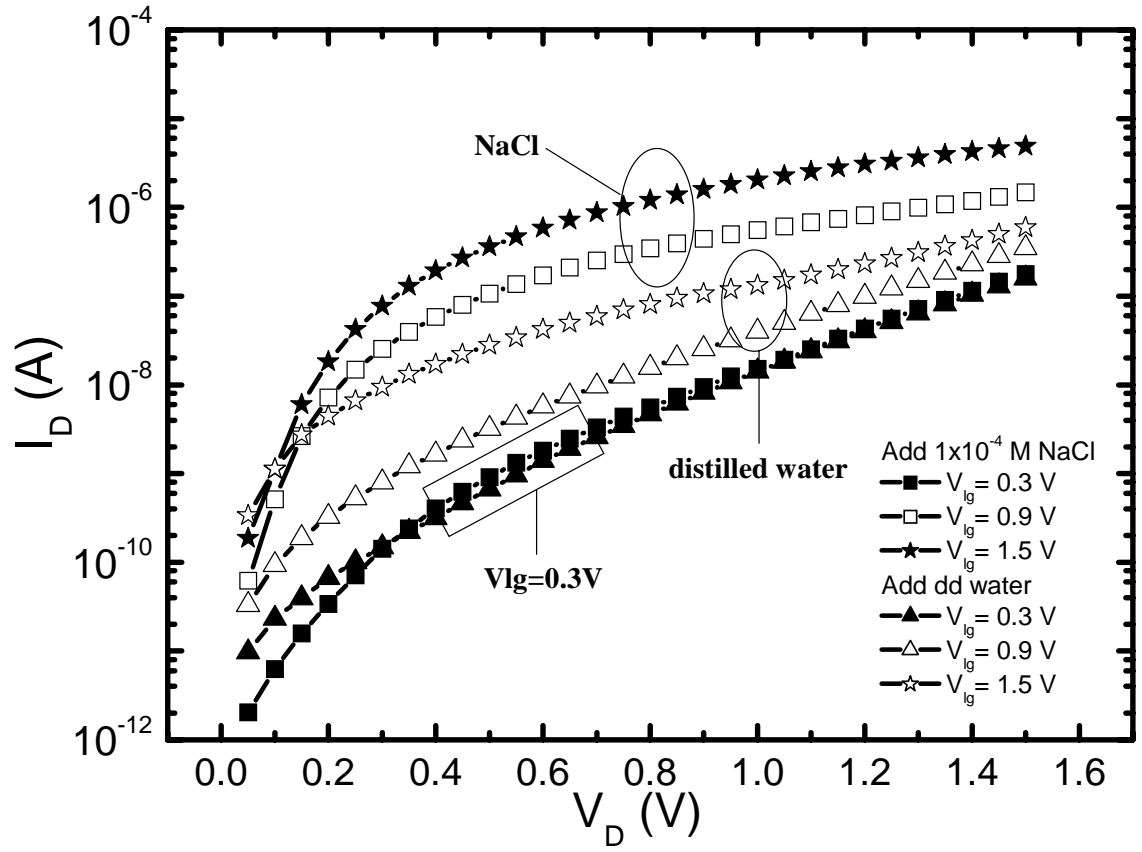


Figure 25. I-V curves illustrated the relation between deionized water and NaCl solutions. The measured drain current for CNTs exposed to the distilled water (\blacktriangle for $V_{lg} = 0.3$ V, \triangle for $V_{lg} = 0.9$ V, and \star for $V_{lg} = 1.5$ V) and aqueous 1×10^{-4} NaCl solution (\blacksquare for $V_{lg} = 0.3$ V, \square for $V_{lg} = 0.9$ V, and \star for $V_{lg} = 1.5$ V).

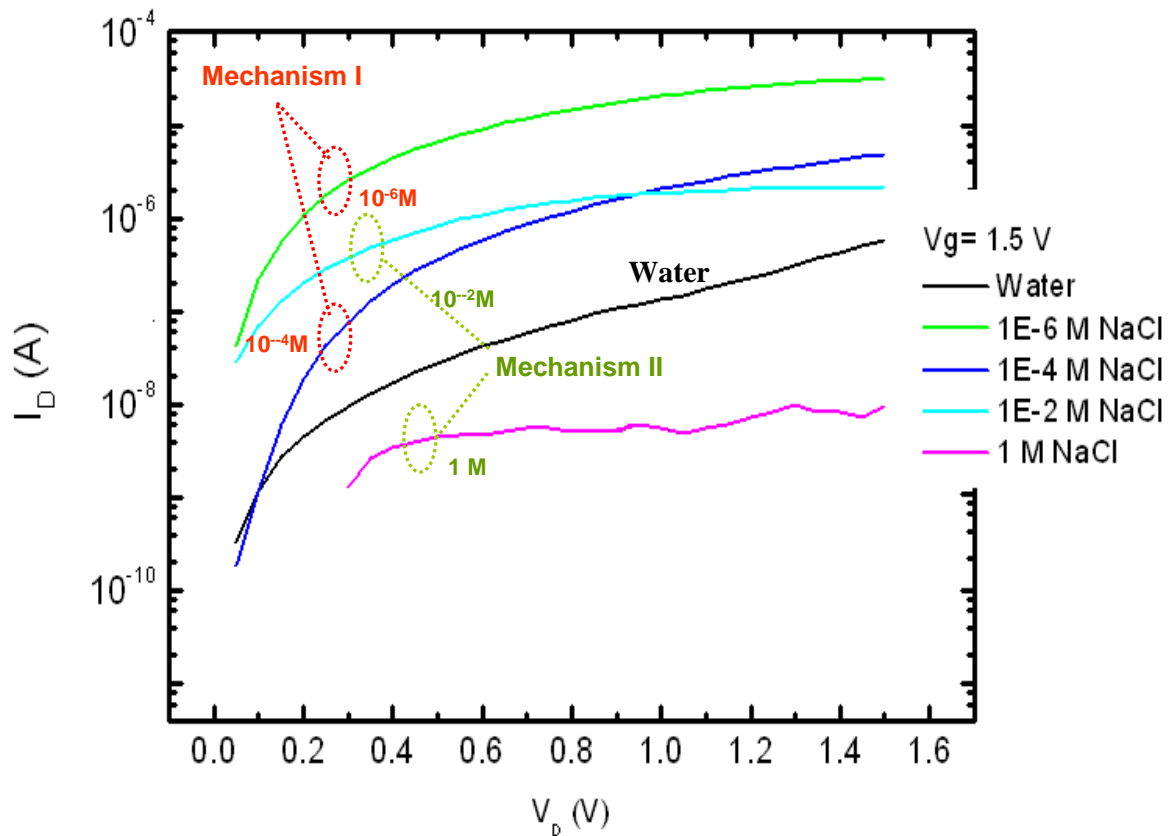


Figure 26. I-V curves illustrated different concentration curves of NaCl solution.

The liquid-gate voltage was kept constant at 1.5V for the measurement. Data for the distilled water (black line), 1×10^{-6} M NaCl solution (green line), 1×10^{-4} M NaCl solution (mazarine line), 1×10^{-2} M NaCl solution (blue line), 1 M NaCl solution (purple line). It was divided into two groups by the fashion of curves. The mechanism I includes 1×10^{-6} M and 1×10^{-4} M NaCl solution, and the mechanism II includes 1×10^{-2} M and 1 M NaCl solution.